Critical bed shear for initial movement of sediments on a combined lateral and longitudinal slope

Subhasish Dey

Associate Professor, Department of Civil Engineering, Indian Institute of Technology, Kharagpur 721302, West Bengal, India.

Tel.: + 91 3222 2832418. Fax: + 91 3222 282254. E-mail: *sdey@civil.iitkgp.ernet.in*

Received 3 October 2002; accepted in revised form 11 August 2003

Abstract An experimental study on critical bed shear-stress for initial movement of non-cohesive sediment particles under a steady-uniform stream flow on a combined lateral (across the flow direction) and longitudinal (streamwise direction) sloping bed is presented. The aim of this paper is to ascertain that the critical bed shear-stress on a combined lateral and longitudinal sloping bed is adequately represented by the product of critical bed shear-stress ratios for lateral and longitudinal sloping beds. Experiments were carried out with closed-conduit flow, in two ducts having a semicircular invert section, with three sizes of sediments. In laboratory flumes, the uniform flow is a difficult – if not impossible – proposition for a steeply sloping channel, and is impossible to obtain in an adversely sloping channel. To avoid this problem, the experiments were conducted with a closed-conduit flow. The critical bed shear-stresses for experimental runs were estimated from side-wall correction. The experimental data agree satisfactorily with the results obtained from the proposed formula.

Keywords Sediment transport; sediment threshold; sediment motion; open channel flow; steady flow; fluvial hydraulics

Nordic Hydrology **Vol 35 No 2 pp 153–164** © IWA Publishing 2004

Introduction

Sediment particles begin to move if a situation is eventually reached when the hydrodynamic forces induced by the flow exceed a certain limiting value. The condition just sufficient to initiate sediment motion is termed the *threshold* or *critical condition*. The pioneering work of Shields (1936) described the initial movement of uniform sediment particles under a unidirectional stream flow on bed slopes close to zero, and hence it cannot be used in channels having substantial bed slopes. The effect of lateral (across the flow direction) or side slopes (α = lateral bed angle with the horizontal) on the threshold of sediment motion was studied by Forchheimer (1924), Fan (1947), Glover and Florey (1951), Lane (1955), Li *et al.* (1976) and Ikeda (1982). On the other hand, the initial movement of sediment on longitudinal (streamwise direction) slopes (θ = longitudinal bed angle with the horizontal) was studied by Luque and van Beek (1976), Whitehouse and Hardisty (1988), Chiew and Parker (1994), Damgaard *et al.* (1996) and Dey *et al.* (1999).

Forchheimer (1924) was the first to provide a concept of three-dimensional analysis of the gravity and drag forces on particles resting on the lateral slopes of channels, at the state of threshold motion. Fan (1947) developed a detailed analysis of a channel section using the concept of Forchheimer. A similar analysis was also given independently by the US Bureau of Reclamation under the direction of Lane (1955), to develop an equation of critical bed shear-stress ratio as a function of side slope and angle-of-repose of bed sediments. Lane's work was extended by Li *et al.* (1976) for a channel in coarse alluvium. Considering the sediment particles on the side slopes of the channel to be at a critical condition, Glover and Florey (1951) proposed the profile of a minimum stable cross-section of a channel. Ikeda (1982) developed the equation of critical bed shear-stress ratio for the threshold of sediment particle motion on side slopes, considering the equilibrium of a sediment particle, and

conducted experiments to verify the equation. Dey (2001) applied Ikeda's work to propose a mathematical model for a threshold channel, assuming sediment particles are at a critical condition on the side slopes of a channel.

In longitudinal sloping beds, limited experiments by Luque and van Beek (1976) showed that the critical bed shear-stress required for the initial movement of sediment decreases with increase in slope. Whitehouse and Hardisty (1988) carried out experiments on adverse and streamwise longitudinal bed slopes to examine the effect of slopes and angle-of-repose on critical bed shear-stress. Chiew and Parker (1994) conducted experiments to determine the critical bed shear-stress for the beginning of sediment motion in closed-conduits having adverse and streamwise longitudinal slopes. Dey *et al.* (1999) gave a theoretical model for the estimation of critical bed shear-stress on longitudinal sloping beds, considering the equilibrium of a solitary particle. They expressed critical bed shear-stress in terms of particle Reynolds number and angle-of-repose of sediment particles. Dey and Debnath (2000) conducted experiments to verify the theoretical model developed by Dey *et al.* (1999). More of these studies have been reported elsewhere (Stevens *et al.* 1976; Howard 1977; Allen 1982; Dyer 1986; Sarre 1987; Iversen and Rasmussen 1994; Damgaard *et al.* 1996).

Little attention has so far been given to formulating the critical bed shear-stress required for the initial movement of sediment on a combined lateral and longitudinal sloping bed. Most of the rivers have complex three-dimensional topography, with lateral and longitudinal sloping beds in most of the cross-sections. This type of bed slope is particularly common in hilly rivers in hilly areas, meandering rivers, and coastal and estuarine morphologies. Therefore, it is important to quantify the bed shear-stress that is responsible for the initial movement of sediment on combined sloping beds, which can be applicable to both channel beds and banks.

The aim of this paper is to ascertain whether the product of critical bed shear-stress ratios for lateral and longitudinal sloping beds is adequate to represent the critical bed shear-stress on a combined lateral and longitudinal sloping bed. To verify this, experiments were carried out in two semicircular inverted ducts (closed-conduit flow) with three types of sediments.

Formulation

For lateral sloping beds, Lane (1955) derived the following equation for the critical bed shear-stress ratio K_α:

$$K_\alpha = \frac{\tau_\alpha}{\tau_o} = \sqrt{1 - \frac{\sin^2\alpha}{\sin^2\phi}} \tag{1}$$

where τ_α = critical bed shear-stress on a lateral sloping bed, τ_o = critical bed shear-stress on a horizontal bed and ϕ = angle-of-repose of bed sediments. Ikeda (1982) also obtained the same equation while studying the initial movement of sediment on lateral slopes.

On the other hand, for longitudinal sloping beds, the critical bed shear-stress ratio K_θ is given by:

$$K_\theta = \frac{\tau_\theta}{\tau_o} = \cos\theta\left(1 - \frac{\tan\theta}{\tan\phi}\right) \tag{2}$$

To determine critical bed shear-stress for sediment particles on a longitudinal sloping bed, Luque and van Beek (1976), Stevens *et al.* (1976), Howard (1977), Allen (1982), Whitehouse and Hardisty (1988), Chiew and Parker (1994), Iversen and Rasmussen (1994), Dey *et al.* (1999) and Dey and Debnath (2000) used relationships similar to that of Eq. (2).

Combining Eqs (1) and (2), the equation of critical bed shear-stress ratio K on a combined lateral and longitudinal sloping bed can be proposed as:

$$K = \frac{\tau_{\alpha\theta}}{\tau_o} = K_\theta K_\alpha \tag{3}$$

where $\tau_{\alpha\theta}$ = critical bed shear-stress on a combined lateral and longitudinal sloping bed. There are always inherent difficulties in carrying out the experiments on steep or adverse slopes in a laboratory flume. For the steep bed slopes, the flow is difficult to control, and, consequently, the uniform flow is very difficult to establish. On the other hand, it is impossible to achieve uniform flow in adversely sloping channels. Moreover, in the present case, a lateral slope also exists. To avoid these difficulties, the experiments are conducted in semicircular inverted ducts (closed-conduit flow), wherein it is rather easy to alter the bed slopes to any desired value while maintaining a uniform flow.

Experimental set-up and procedure

Experiments were conducted in two Perspex semicircular inverted ducts (flat base downward) (Fig. 1) – one with a diameter of 67.5 mm (duct 1) and the other with a diameter of 30.5 mm (duct 2). The lengths of the ducts were both 3.5 m. The transparent Perspex wall enabled observations to be made of the movement of the sediment particles. A flexible joint allowing the bed slopes to be changed to any desired value connected the duct to an upstream water supply. Water was discharged through the downstream end of the duct into a measuring tank. A valve in the upstream water supply-line controlled the discharge of water. Another valve was also installed downstream of the duct to allow a finer adjustment of the discharge. The lateral and longitudinal slopes were varied from 0° to 25° and − 15° (upslope) to 25° (downslope), respectively. A sediment trap, where sediments were kept for testing, was constructed 2.5 m downstream of the inlet of the duct in order to obtain a fully developed flow. The sediment trap was 0.15 m long and 5 mm deep below the floor of the duct. The flow was uniform in the sediment-trap portion, as it was fully developed. Sediment particles of an appropriate size were glued on the surface of the floor in order to simulate the roughness of the sediment bed. Altogether, three uniform sediments were tested in this study. The geometric standard deviation σ_g of the particle-size distribution, given by $\sqrt{d_{84}/d_{16}}$, is less

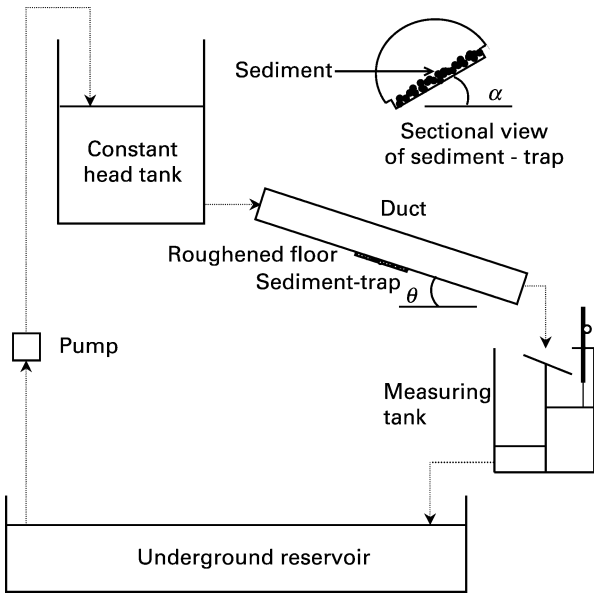

Figure 1 Experimental set-up

than 1.4 for uniform sediments (Dey *et al.* 1995). Table 1 shows the properties of the sediments used in the experiment.

The sediments were inserted in the sediment trap by a flexible tube inserted through a porthole at the top of the duct. After filling the sediment trap with the sediments, the bed was perfectly leveled to give a continuous surface along the floor without any perturbation. The leveling was done by inserting a flat, thin steel plate through the downstream opening of the duct. Then, at the downstream opening, the downstream valve was attached and the duct was held firmly by a suitable holding arrangement, giving a predetermined bed (floor) slope in both the lateral and longitudinal directions. The upstream valve was slightly opened to allow water to completely fill the duct. The downstream valve was then opened gradually and close observations were made of the movement of the sediment particles. The discharge was increased by slowly opening the upstream valve until the sediment particles started to move on the bed surface over a period of time. It is difficult to observe the real beginning of sediment movement (Neill and Yalin 1969). However, only a certain degree of established movement of sediment can be considered as the critical condition of sediment motion. Once the critical condition had been reached, the corresponding discharge was registered, with the aid of a measuring tank.

Determination of critical bed shear-stress

The bed shear-stress τ_b as a function of dynamic pressure is given by:

$$\tau_b = \frac{f_b}{8}\rho V_b^2 \tag{4}$$

where $f =$ friction factor, $\rho =$ mass density of water and $V =$ mean velocity of flow. Subscript b refers to the quantities associated with the bed. The Colebrook–White equation, used to evaluate f_b, is:

$$\frac{1}{\sqrt{f_b}} = -0.86\ \ln\left(\frac{k_s P_b}{14.8A_b} + \frac{2.51}{R_b\sqrt{f_b}}\right) \tag{5}$$

where $k_s =$ equivalent roughness height, $A =$ flow area, $P =$ wetted perimeter and $R =$ Reynolds number of flow.

In this study, the bed is rough (consisting of sediment particles) and the semicircular wall is smooth. Therefore, f_w is considerably different from f_b, where subscript w refers to the quantities associated with the semicircular wall. As a result of this, τ_w is significantly different from τ_b. Vanoni's (1975) method of *side-wall correction* is applied in this study, due to the smooth wall and rough bed for a cross-section of the duct. Using the continuity equation, the discharge Q is expressed as:

$$Q = AV = A_w V_w + A_b V_b \tag{6}$$

The mean velocity, V, being the same as V_w and V_b (Vanoni 1975), can be obtained once Q is known. The equation of force along the streamwise direction is given by:

Table 1 Properties of sediments used in experiments

d_{50} (mm)	Relative density (s)	σ_g	τ_o (Pa)	ϕ (deg)
0.60	2.65	1.39	0.591	32
0.94	2.65	1.21	0.978	34
1.35	2.65	1.38	1.510	35

$$-A\frac{\mathrm{d}p}{\mathrm{d}x} = \rho\frac{f}{8}V^2P = \rho\frac{f_\mathrm{w}}{8}V_\mathrm{w}^2P_\mathrm{w} + \rho\frac{f_\mathrm{b}}{8}V_\mathrm{b}^2P_\mathrm{b} \tag{7}$$

where $\mathrm{d}p/\mathrm{d}x$ = streamwise pressure gradient. Using $V = V_\mathrm{w} = V_\mathrm{b}$ into Eq. (7), one obtains:

$$Pf = P_\mathrm{w}f_\mathrm{w} + P_\mathrm{b}f_\mathrm{b} \tag{8}$$

As the piezometric head is the same for both the smooth wall and the rough bed regions, equating the static pressure force at the wall and bed regions, one obtains:

$$\frac{Pf}{A} = \frac{P_\mathrm{w}f_\mathrm{w}}{A_\mathrm{w}} = \frac{P_\mathrm{b}f_\mathrm{b}}{A_\mathrm{b}} \tag{9}$$

The Reynolds numbers of flow for different regions are given by:

$$R = \frac{4VA}{\nu P}, R_\mathrm{w} = \frac{4VA_\mathrm{w}}{\nu P_\mathrm{w}}, R_\mathrm{b} = \frac{4VA_\mathrm{b}}{\nu P_\mathrm{b}} \tag{10}$$

where ν = the kinematic viscosity of fluid. Substituting Eq. (9) into Eq. (8), one can write:

$$\frac{R}{f} = \frac{R_\mathrm{w}}{f_\mathrm{w}} = \frac{R_\mathrm{b}}{f_\mathrm{b}} \tag{11}$$

As the wall is smooth, the Blasius equation can be used to evaluate f_w. It is

$$f_\mathrm{w} = \frac{0.316}{R_\mathrm{w}^{0.25}} \tag{12}$$

Using Eqs (6)–(12), the following equation is obtained as:

$$f_\mathrm{b} = 0.316R_\mathrm{b}\left(\frac{4VA}{\nu P_\mathrm{w}} - \frac{R_\mathrm{b}P_\mathrm{b}}{P_\mathrm{w}}\right)^{-1.25} \tag{13}$$

Again, substituting Eq. (5) into Eq. (13), the Colebrook–White equation becomes:

$$\frac{1}{\sqrt{f_\mathrm{b}}} = -0.86\ \ln\left(\frac{k_\mathrm{s}V}{3.7\nu R_\mathrm{b}} + \frac{2.51}{R_\mathrm{b}\sqrt{f_\mathrm{b}}}\right) \tag{14}$$

Here, the equivalent roughness height k_s is assumed to be the mean size of sediment d_{50}, as was done by Wiberg and Smith (1987), Dey (1999) and Dey and Debnath (2000). For the given data for V, P, P_w, P_b, ν, ρ and d_{50}, the values of R_b and f_b can be evaluated numerically by solving Eqs (13) and (14). Then, Eq. (4) is used to determine bed shear-stress τ_b. The value of τ_b for a critical state of sediment motion for a combined lateral and longitudinal sloping bed is $\tau_{\alpha\theta}$, as given in Eq. (3).

Experimental results

The experimental critical bed shear-stresses $\tau_{\alpha\theta}$ were determined using the methodology described in the preceding section, for various samples of sediments and various bed slopes. However, the computed values of K were obtained from Eq. (3). Tables 2(a) and 2(b) present the experimental data of the initial movement of sediment on combined lateral and longitudinal sloping beds collected in ducts 1 and 2. Fig 2 shows the comparison of the results of K obtained using Eq. (3) with the present experimental data. The values of critical bed shear-stress τ_o ($\alpha = \theta = 0$) on a horizontal bed for different sediments (given in Table 1) that were being used to normalize the experimental values of $\tau_{\alpha\theta}$, were obtained experimentally in ducts 1 and 2. In Fig. 2, the experimental data agree satisfactorily with the computed results of K obtained using Eq. (2), having a correlation coefficient of 0.965. Also, Figs 3 and 4 present the variation of K/K_α with θ for different values of α. In Figs 3 and 4, the

Table 2(a) Experimental data collected in duct 1

		$d_{50} = 0.60$ mm				$d_{50} = 0.94$ mm				$d_{50} = 1.35$ mm			
θ (deg)	α (deg)	V (m/s)	f_b	$\hat{\tau}_{\alpha\theta}$	K	V (m/s)	f_b	$\hat{\tau}_{\alpha\theta}$	K	V (m/s)	f_b	$\hat{\tau}_{\alpha\theta}$	K
−15	0	0.406	0.043	0.0899	1.476	0.486	0.047	0.0920	1.433	0.574	0.053	0.0991	1.433
−10	0	0.385	0.043	0.0814	1.337	0.459	0.048	0.0820	1.275	0.529	0.053	0.0844	1.221
−5	0	0.357	0.043	0.0706	1.159	0.432	0.048	0.0734	1.141	0.510	0.053	0.0786	1.137
0	0	0.331	0.043	0.0608	0.998	0.403	0.048	0.0640	0.995	0.475	0.053	0.0685	0.991
5	0	0.313	0.043	0.0548	0.900	0.382	0.048	0.0578	0.899	0.446	0.053	0.0605	0.874
10	0	0.292	0.044	0.0481	0.790	0.354	0.048	0.0498	0.775	0.393	0.054	0.0474	0.685
15	0	0.276	0.044	0.0432	0.709	0.318	0.049	0.0405	0.629	0.372	0.054	0.0426	0.617
20	0	0.256	0.044	0.0373	0.612	0.276	0.049	0.0310	0.482	0.314	0.054	0.0307	0.444
25	0	0.212	0.045	0.0262	0.431	0.218	0.050	0.0197	0.306	0.257	0.055	0.0208	0.301
−15	5	0.382	0.043	0.0803	1.318	0.456	0.048	0.0812	1.263	0.544	0.053	0.0892	1.290
−10	5	0.370	0.043	0.0753	1.237	0.441	0.048	0.0763	1.186	0.504	0.053	0.0767	1.109
−5	5	0.342	0.043	0.0648	1.064	0.407	0.048	0.0653	1.015	0.481	0.053	0.0702	1.016
0	5	0.316	0.043	0.0558	0.916	0.383	0.048	0.0586	0.911	0.446	0.053	0.0607	0.878
5	5	0.293	0.043	0.0484	0.795	0.362	0.048	0.0521	0.809	0.427	0.053	0.0558	0.806
10	5	0.274	0.044	0.0425	0.698	0.338	0.049	0.0456	0.709	0.377	0.054	0.0437	0.632
15	5	0.265	0.044	0.0399	0.656	0.229	0.049	0.0359	0.559	0.350	0.054	0.0379	0.549
20	5	0.241	0.044	0.0333	0.546	0.261	0.050	0.0276	0.430	0.294	0.055	0.0270	0.391
25	5	0.198	0.045	0.0231	0.380	0.208	0.051	0.0180	0.280	0.242	0.055	0.0185	0.268
−15	10	0.370	0.043	0.0753	1.237	0.430	0.048	0.0727	1.130	0.522	0.053	0.0821	1.189
−10	10	0.347	0.043	0.0668	1.097	0.415	0.048	0.0668	1.038	0.479	0.053	0.0695	1.005
−5	10	0.320	0.043	0.0570	0.937	0.391	0.048	0.0604	0.940	0.456	0.053	0.0632	0.914
0	10	0.294	0.044	0.0484	0.795	0.316	0.048	0.0517	0.804	0.430	0.053	0.0565	0.817
5	10	0.284	0.044	0.0456	0.749	0.341	0.049	0.0462	0.719	0.401	0.054	0.0493	0.714
10	10	0.265	0.044	0.0400	0.657	0.320	0.049	0.0410	0.636	0.354	0.054	0.0387	0.560
15	10	0.251	0.044	0.0360	0.590	0.301	0.049	0.0365	0.568	0.343	0.054	0.0365	0.527
20	10	0.229	0.045	0.0300	0.492	0.279	0.049	0.0314	0.489	0.316	0.054	0.0311	0.487
25	10	0.188	0.046	0.0208	0.342	0.228	0.050	0.0214	0.332	0.263	0.055	0.0218	0.316
−15	15	0.349	0.043	0.0676	1.109	0.418	0.048	0.0686	1.067	0.490	0.053	0.0727	1.052

Table 2(a) – *continued*

		d_{50} = 0.60 mm				d_{50} = 0.94 mm				d_{50} = 1.35 mm			
θ (deg)	α (deg)	V (m/s)	f_b	$\hat{\tau}_{\alpha\theta}$	K	V (m/s)	f_b	$\hat{\tau}_{\alpha\theta}$	K	V (m/s)	f_b	$\hat{\tau}_{\alpha\theta}$	K
−10	15	0.329	0.043	0.0602	0.988	0.389	0.048	0.0597	0.928	0.451	0.053	0.0620	0.896
−5	15	0.308	0.044	0.0530	0.870	0.368	0.048	0.0536	0.834	0.430	0.053	0.0565	0.818
0	15	0.279	0.044	0.0438	0.720	0.341	0.049	0.0462	0.719	0.405	0.054	0.0503	0.727
5	15	0.265	0.044	0.0398	0.653	0.328	0.049	0.0430	0.669	0.380	0.054	0.0443	0.642
10	15	0.248	0.044	0.0352	0.578	0.297	0.049	0.0357	0.555	0.342	0.054	0.0361	0.523
15	15	0.235	0.045	0.0317	0.521	0.283	0.049	0.0325	0.505	0.327	0.054	0.0331	0.479
20	15	0.224	0.045	0.0290	0.477	0.266	0.050	0.0287	0.447	0.307	0.055	0.0292	0.423
25	15	0.177	0.046	0.0187	0.306	0.223	0.050	0.0205	0.318	0.253	0.055	0.0202	0.293
−15	20	0.329	0.043	0.0603	0.989	0.389	0.048	0.0598	0.930	0.459	0.053	0.0640	0.928
−10	20	0.311	0.043	0.0540	0.887	0.367	0.048	0.0535	0.832	0.430	0.053	0.0565	0.818
−5	20	0.286	0.044	0.0461	0.758	0.363	0.048	0.0525	0.818	0.418	0.053	0.0534	0.772
0	20	0.265	0.044	0.0398	0.639	0.323	0.049	0.0417	0.648	0.380	0.054	0.0444	0.642
5	20	0.243	0.045	0.0339	0.556	0.301	0.049	0.0364	0.567	0.362	0.054	0.0403	0.583
10	20	0.234	0.045	0.0315	0.517	0.286	0.049	0.0330	0.513	0.331	0.054	0.0340	0.492
15	20	0.211	0.045	0.0260	0.426	0.263	0.050	0.0282	0.438	0.309	0.054	0.0297	0.430
20	20	0.192	0.046	0.0217	0.356	0.233	0.050	0.0223	0.347	0.268	0.055	0.0226	0.328
25	20					0.208	0.051	0.0179	0.279	0.246	0.055	0.0191	0.276
−15	25	0.301	0.044	0.0509	0.836	0.358	0.048	0.0509	0.792	0.431	0.053	0.0566	0.819
−10	25	0.294	0.044	0.0485	0.797	0.352	0.048	0.0429	0.668	0.402	0.054	0.0495	0.716
−5	25	0.263	0.044	0.0393	0.646	0.324	0.049	0.0421	0.655	0.383	0.054	0.0450	0.651
0	25	0.243	0.045	0.0339	0.556	0.300	0.049	0.0362	0.563	0.356	0.054	0.0392	0.567
5	25	0.240	0.045	0.0331	0.538	0.287	0.049	0.0333	0.518	0.334	0.054	0.0346	0.501
10	25	0.218	0.045	0.0275	0.451	0.266	0.050	0.0287	0.446	0.308	0.054	0.0295	0.426
15	25	0.188	0.046	0.0209	0.344	0.241	0.050	0.0237	0.369	0.284	0.054	0.0252	0.365
20	25					0.220	0.050	0.0201	0.312	0.263	0.055	0.0218	0.316

Table 2(b) Experimental data collected in duct 2

		d_{50} = 0.60 mm				d_{50} = 0.94 mm				d_{50} = 1.35 mm			
θ (deg)	α (deg)	V (m/s)	f_b	$\hat{\tau}_{\alpha\theta}$	K	V (m/s)	f_b	$\hat{\tau}_{\alpha\theta}$	K	V (m/s)	f_b	$\hat{\tau}_{\alpha\theta}$	K
−15	0	0.350	0.057	0.0898	1.475	0.423	0.065	0.0953	1.482	0.502	0.073	0.1048	1.516
−10	0	0.322	0.058	0.0769	1.264	0.389	0.065	0.0810	1.26	0.451	0.073	0.0851	1.232
−5	0	0.304	0.058	0.0690	1.132	0.381	0.065	0.0776	1.207	0.438	0.073	0.0804	1.164
0	0	0.285	0.058	0.0609	1.000	0.349	0.066	0.0645	1.004	0.406	0.074	0.0698	1.010
5	0	0.267	0.059	0.0538	0.884	0.324	0.066	0.0570	0.886	0.395	0.074	0.0627	0.907
10	0	0.249	0.059	0.0472	0.775	0.293	0.066	0.0468	0.728	0.366	0.074	0.0568	0.822
15	0	0.237	0.059	0.0431	0.708	0.264	0.067	0.0383	0.595	0.324	0.075	0.0450	0.651
20	0	0.217	0.060	0.0363	0.597	0.236	0.068	0.0311	0.483	0.255	0.076	0.0283	0.409
25	0	0.187	0.061	0.0274	0.449	0.185	0.069	0.0195	0.302	0.211	0.077	0.0197	0.285
−15	5	0.332	0.057	0.0815	1.338	0.402	0.065	0.0863	1.343	0.477	0.073	0.0950	1.374
−10	5	0.306	0.058	0.0698	1.146	0.370	0.065	0.0735	1.143	0.428	0.074	0.0771	1.117
−5	5	0.289	0.058	0.0624	1.026	0.361	0.065	0.0702	1.092	0.416	0.074	0.0729	1.055
0	5	0.271	0.059	0.0553	0.907	0.329	0.066	0.0584	0.909	0.391	0.074	0.0647	0.936
5	5	0.254	0.059	0.0490	0.804	0.308	0.066	0.0517	0.804	0.366	0.074	0.0568	0.822
10	5	0.237	0.059	0.0429	0.704	0.278	0.067	0.0423	0.658	0.348	0.074	0.0515	0.746
15	5	0.226	0.060	0.0391	0.642	0.250	0.067	0.0347	0.54	0.308	0.075	0.0408	0.590
20	5	0.206	0.060	0.0331	0.543	0.224	0.068	0.0282	0.438	0.242	0.076	0.0256	0.370
25	5	0.177	0.061	0.0249	0.408	0.175	0.070	0.0176	0.274	0.201	0.078	0.0179	0.259
−15	10	0.315	0.058	0.0736	1.208	0.381	0.065	0.0778	1.211	0.415	0.073	0.0854	1.235
−10	10	0.290	0.058	0.0630	1.034	0.350	0.066	0.0661	1.028	0.406	0.074	0.0694	1.003
−5	10	0.274	0.058	0.0565	0.819	0.343	0.066	0.0634	0.986	0.394	0.074	0.0655	0.948
0	10	0.257	0.059	0.0499	0.819	0.311	0.066	0.0527	0.819	0.371	0.074	0.0583	0.844
5	10	0.241	0.059	0.0441	0.725	0.292	0.067	0.0466	0.724	0.374	0.075	0.0512	0.741
10	10	0.224	0.060	0.0387	0.636	0.263	0.067	0.0381	0.593	0.329	0.075	0.0463	0.671
15	10	0.214	0.060	0.0354	0.580	0.237	0.068	0.0314	0.488	0.292	0.075	0.0368	0.531
20	10	0.195	0.061	0.0298	0.489	0.213	0.068	0.0254	0.395	0.229	0.077	0.0231	0.334
25	10	0.168	0.062	0.0225	0.369	0.192	0.069	0.0210	0.326	0.217	0.077	0.0207	0.301
−15	15	0.297	0.058	0.0658	1.080	0.360	0.065	0.0697	1.084	0.427	0.074	0.0765	1.107

Table 2(b) – *continued*

		d_{50} = 0.60 mm				d_{50} = 0.94 mm				d_{50} = 1.35 mm			
θ (deg)	α (deg)	V (m/s)	f_b	$\hat{\tau}_{\alpha\theta}$	K	V (m/s)	f_b	$\hat{\tau}_{\alpha\theta}$	K	V (m/s)	f_b	$\hat{\tau}_{\alpha\theta}$	K
−10	15	0.274	0.058	0.0565	0.928	0.331	0.066	0.0593	0.923	0.383	0.074	0.0621	0.899
−5	15	0.259	0.059	0.0506	0.831	0.324	0.066	0.0568	0.883	0.372	0.074	0.0589	0.852
0	15	0.242	0.059	0.0448	0.735	0.294	0.067	0.0472	0.734	0.350	0.074	0.0521	0.753
5	15	0.227	0.060	0.0395	0.649	0.276	0.067	0.0418	0.649	0.327	0.075	0.0458	0.663
10	15	0.212	0.060	0.0348	0.572	0.270	0.067	0.0400	0.623	0.311	0.075	0.0416	0.602
15	15	0.202	0.061	0.0318	0.522	0.242	0.068	0.0326	0.508	0.276	0.076	0.0329	0.477
20	15	0.185	0.061	0.0269	0.441	0.226	0.068	0.0285	0.443	0.267	0.076	0.0308	0.446
25	15	0.159	0.062	0.0202	0.332	0.198	0.069	0.0223	0.346	0.217	0.077	0.0208	0.301
−15	20	0.280	0.058	0.0587	0.964	0.339	0.066	0.0619	0.962	0.401	0.074	0.0679	0.983
−10	20	0.258	0.059	0.0504	0.827	0.311	0.066	0.0527	0.819	0.361	0.074	0.0553	0.800
−5	20	0.244	0.059	0.0452	0.743	0.304	0.066	0.0505	0.784	0.350	0.074	0.0521	0.753
0	20	0.228	0.060	0.0399	0.656	0.276	0.067	0.0420	0.653	0.329	0.075	0.0463	0.671
5	20	0.214	0.060	0.0354	0.580	0.259	0.067	0.0371	0.576	0.308	0.075	0.0408	0.590
10	20	0.200	0.061	0.0311	0.510	0.234	0.068	0.0306	0.476	0.293	0.075	0.0369	0.534
15	20	0.180	0.061	0.0255	0.419	0.215	0.068	0.0260	0.404	0.254	0.076	0.0281	0.407
20	20	0.158	0.062	0.0201	0.330	0.189	0.069	0.0203	0.316	0.223	0.077	0.0219	0.317
25	20					0.161	0.069	0.0150	0.234	0.185	0.078	0.0154	0.222
−15	25	0.262	0.059	0.059	0.853	0.318	0.066	0.0547	0.851	0.376	0.074	0.0600	0.868
−10	25	0.241	0.059	0.059	0.732	0.292	0.067	0.0466	0.724	0.338	0.075	0.0487	0.705
−5	25	0.228	0.060	0.060	0.656	0.285	0.067	0.0447	0.695	0.329	0.075	0.0462	0.667
0	25	0.214	0.060	0.060	0.580	0.260	0.067	0.0372	0.579	0.309	0.075	0.0409	0.592
5	25	0.200	0.061	0.061	0.513	0.243	0.068	0.0328	0.51	0.289	0.075	0.0360	0.521
10	25	0.183	0.061	0.061	0.433	0.219	0.068	0.0270	0.42	0.275	0.076	0.0327	0.473
15	25	0.166	0.062	0.062	0.362	0.199	0.069	0.0224	0.348	0.236	0.077	0.0243	0.351
20	25					0.186	0.069	0.0197	0.306	0.217	0.077	0.0208	0.301

Note: $\hat{\tau}_{\alpha\theta}$ is the non-dimensional $\tau_{\alpha\theta}$ expressed as $\tau_{\alpha\theta}/[(\rho_s-\rho)gd_{50}]$, where ρ_s = mass density of sediment.

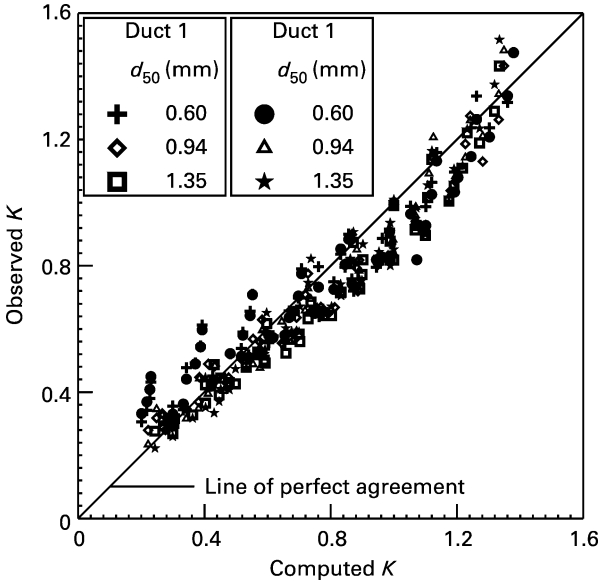

Figure 2 Comparison of the experimental data with the results obtained using Eq. (3)

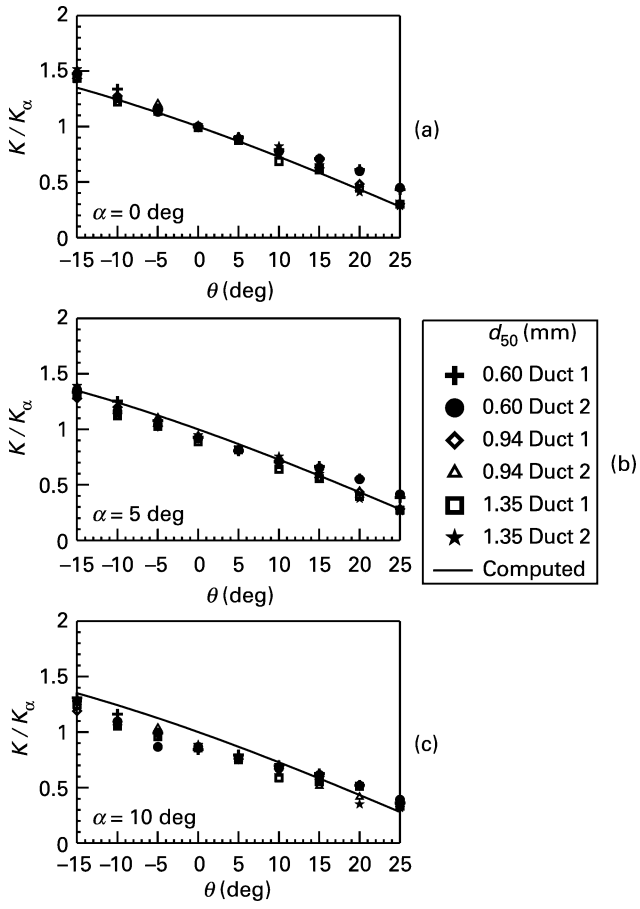

Figure 3 Variation of K/K_α with θ for (a) $\alpha = 0°$, (b) $\alpha = 5°$ and (c) $\alpha = 10°$

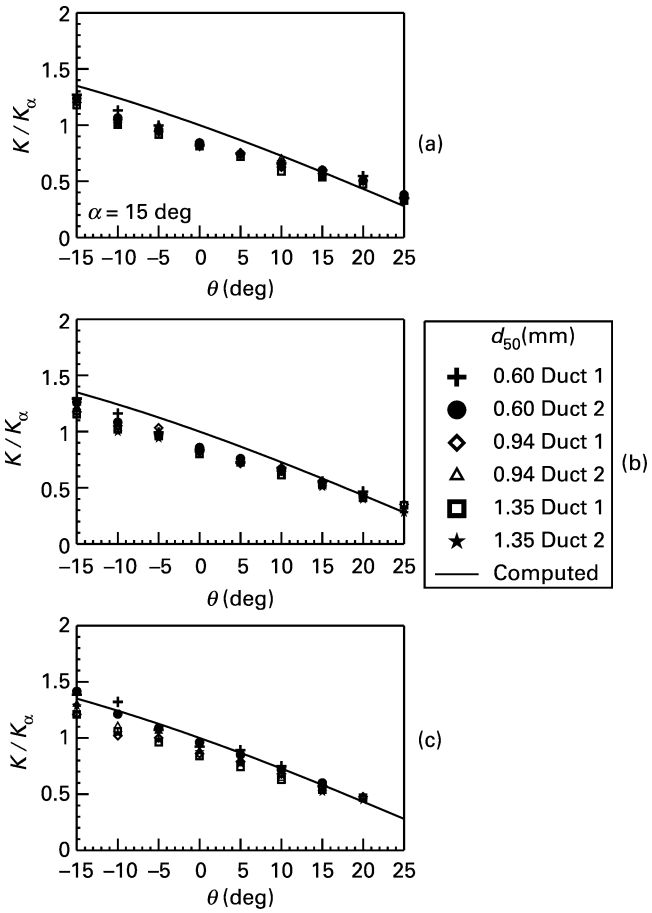

Fig. 4 Variation of K/K_α with θ for (a) $\alpha = 15°$, (b) $\alpha = 20°$ and (c) $\alpha = 25°$

computed curves obtained from Eq. (3) using an average value of $\phi = 34°$, correspond closely with the experimental data. Thus, the present study confirms that Eq. (3) can adequately describe the critical bed shear-stress for the initial movement of sediment on a combined lateral and longitudinal sloping bed. However, in the present study, the variation of uniform sediment size d_{50} was taken as 0.60–1.35 mm. Therefore, experiments on the initial movement of sediment with larger particle sizes ($d_{50} > 1.5$ mm) and non-uniform sediments would be worthwhile considering for future research.

Conclusions

Critical bed shear-stress on a combined lateral and longitudinal sloping bed can be represented adequately by the product of critical bed shear-stress ratios for lateral and longitudinal sloping beds. Experiments were conducted in two ducts (closed-conduit flow) having a semicircular inverted section, using three sizes of sediments. The results obtained from the formulation correspond closely with the experimental results.

References

Allen, J.R.L. (1982). Simple models for the shape and symmetry of tidal sand wave: (1) statically stable equilibrium forms. *Mar. Geol.*, **48**, 31–49.

Chiew, Y.M. and Parker, G. (1994). Incipient sediment motion on non-horizontal slopes. *J. Hydraul. Res.*, **32**(5), 649–660.

Damgaard, J.S., Whitehouse, R.J.S. and Wallingford, H.R. (1996). Gravity effects in bed-load sediment transport. *Progress Report, MAFF Contract CSA 3051*, Ministry of Agriculture, Fisheries and Food, London, UK.

Dey, S. (1999). Sediment threshold. *Appl. Math. Modelling*, **23**(5), 399–417.

Dey, S. (2001). Bank profile of threshold channels: a simplified approach. *J. Irrig. Drain. Engrg, ASCE*, **127**(3), 184–187.

Dey, S. and Debnath, K. (2000). Influence of stream-wise bed slope on sediment threshold under stream flow. *J. Irrig. Drain. Engrg, ASCE*, **126**(4), 255–263.

Dey, S., Bose, S.K. and Sastry, G.L.N. (1995). Clear water scour at circular piers: a model. *J. Hydraul. Engrg, ASCE*, **121**(12), 869–876.

Dey, S., Sarker, H.K. and Debnath, K. (1999). Sediment threshold under stream flow on horizontal and sloping beds. *J. Engrg. Mech., ASCE*, **125**(5), 545–553.

Dyer, K.R. (1986). *Coastal and Estuarine Sediment Dynamics*, Wiley, London.

Fan, C.H. (1947). A study of stable channel cross section. *J. Hydraul. Engrg, Chinese Soc. Hydraul. Engrs*, **15**(1), 71–79.

Forchheimer, P. (1924). *Hydraulik*. Teubner Verlagsgesellschaft, Berlin, Germany.

Glover, R.E. and Florey, Q.L. (1951). Stable channel profiles. *Hydraul. Lab. Rep. Hyd-325*, US Bureau of Reclamation, Washington DC, USA.

Howard, A.D. (1977). Effect of slope on the threshold of motion and its application to orientation of wind ripples. *Bull. Geol. Soc. Am.*, **88**, 853–856.

Ikeda, S. (1982). Incipient motion of sand particles on side slopes. *J. Hydraul. Div., ASCE*, **108**(1), 95–114.

Iversen, J.D. and Rasmussen, K.R. (1994). The effect of surface slope on saltation threshold. *Sedimentology*, **41**, 721–728.

Lane, E.W. (1955). Design of stable channels. *Trans. ASCE*, **120**, 1234–1260.

Li, R., Simons, D.B. and Stevens, M.A. (1976). Morphology of cobble streams in small watersheds. *J. Hydraul. Div., ASCE*, **102**(8), 1101–1117.

Luque, R.F. and van Beek, R. (1976). Erosion and transport of bed-load sediment. *J. Hydraul. Res.*, **14**(2), 127–144.

Neill, C.R. and Yalin, M.S. (1969). Quantitative definition of beginning of bed movement. *J. Hydraul. Div., ASCE*, **95**(1), 585–588.

Sarre, R.D. (1987). Aeolian sand transport. *Progr. Phys. Geogr.*, **11**, 157–182.

Shields, A. (1936). Anwendung der aehnlichkeitsmechanik und der turbulenzforschung auf die geschiebebewegung. *Mitteilungen der Preussischen Versuchsanstalt für Wasserbau und Schiffbau*, **26**, Berlin, Germany.

Stevens, M.A., Simons, D.B. and Lewis, G.L. (1976). Safety factor for riprap protection. *J. Hydraul. Engrg., ASCE*, **102**(5), 637–655.

Vanoni, V.A. (1975). *Sedimentation Engineering*. ASCE Manual, No. 54, ASCE, New York, USA.

Whitehouse, R.J.S. and Hardisty, J. (1988). Experimental assessment of two theories for the effect of bed slope on the threshold of bed-load transport. *Mar. Geol.*, **79**, 135–139.

Wiberg, P.L. and Smith, J.D. (1987). Calculations of the critical shear stress for motion of uniform and heterogeneous sediments. *Wat. Resour. Res.*, **23**(8), 1471–1480.